0273-2289/05/121–124/639–652/$30.00

Enhancing Design of Immobilized Enzymatic Microbioreactors Using Computational Simulation

Robert Bailey,*[,1] Frank Jones,[1] Ben Fisher,[1] and Bill Elmore[2]

[1]Chemical, Environmental, and Mechanical Engineering, University of Tennessee at Chattanooga, 615 McCallie Ave. Chattanooga, TN 37403 E-mail: robert.t.bailey@saic.com; and [2]Chemical Engineering Department, Louisiana Tech University, P.O. Box 10348 T.S. Reston, LA 71272

Abstract

In continuous-flow enzymatic microbioreactors, enzymes on the channel walls catalyze reaction(s) among feed chemicals, resulting in the production of some desirable material or the destruction of some undesirable material. Computational models of microbioreactors were developed using the CFD-ACE+ multiphysics simulation package. These models were validated via comparison with experimental data for the destruction of urea, catalyzed by urease. Similar models were then used to assess the impact of internal features on destruction efficiency. It was found that triangular features within the channels enhanced the destruction efficiency more than could be attributed to the increase in surface area alone.

Index Entries: Numerical modeling; microreactor; enzyme; urea; polydimethylsiloxane; destruction efficiency.

Introduction

Miniaturizing traditional engineering process devices and systems has become a growing pursuit in the last decade owing to the many advantages of the small scale, including enhanced heat and mass transfer and scale-up by replication *(1,2)*. These devices are generally fabricated from silicon wafers using the techniques of the microelectronics industry *(3,4)*. Much of the work in this field so far has been devoted to creating and studying the behavior of microchannel-based chemical reactors, mixers, and heat exchangers. However, micromachining silicon is difficult, costly,

*Author to whom all correspondence and reprint requests should be addressed: Science Applications International Corporation, 3465-A Box Hill Corporate Center Drive, Abingdon, MD 21009–1201.

and time-consuming. More recently, microdevices have been made by molding plastics, significantly reducing costs and manufacturing time *(5,6)*.

In previous work, we fabricated continuous-flow biologic microreactors from polydimethylsiloxane (PDMS) consisting of multiple rectangular channels with cross dimensions of 125 × 500 μm. The channels included a regular pattern of molded triangular shapes to serve as packing. Enzymes were immobilized on the surfaces for catalysis (urease was entrapped in the walls during fabrication). The degradation of urea was measured over a variety of catalyst surface populations and flow rates *(7)*.

Experimental testing such as that just described is one way to identify and refine characteristics that lead to improved microreactor performance. Another way is to simulate the processes within microreactors using state-of-the-art computer-modeling techniques. The latter approach has several advantages including the ability to evaluate changes in microreactor configurations with substantially reduced time, effort, and cost. To capitalize on these advantages, investigators have begun to apply computational simulation techniques to microdevices, examining a variety of phenomena including pressure drop, transition to turbulent flow, and heat and mass transfer *(8–12)*. Application of these techniques to enzymatic bioreactors could prove very useful, and with this in mind, we formulated the following three objectives for the present study:

1. Develop computational models of enzymatic microbioreactors, which include all relevant physical processes.
2. Validate the computational models via comparison with experimental data for one enzyme/reaction combination.
3. Use the validated models to predict the effect of a simple design change on reactor performance (destruction efficiency) for other enzyme/reaction combinations.

By accomplishing these three objectives, we intend to demonstrate that computational modeling can be used effectively as a design tool for improving the performance of microbioreactors.

Theory

Governing Equations

The flow and mixing of chemically reacting liquids is described mathematically by a complex set of coupled nonlinear partial differential equations. For the physical situations investigated in our study, five assumptions are introduced that simplify these equations significantly:

1. The density and viscosity of the bulk mixture are determined by the primary constituent, water. The very small concentration of the substrate (urea or hydrogen peroxide) has no appreciable effect on these parameters.

2. The flow is steady and incompressible.
3. Owing to the small cross-sectional area of the microchannels and resultant small Reynolds numbers, the flow is laminar.
4. Chemical reactions take place only at the walls of the reactor channels. There are no homogeneous reactions within the flow field away from the walls.
5. The effects of heat of reaction are negligible owing to the low substrate inlet concentration; thus, the mixture is essentially isothermal.

With these assumptions the flow field (velocity and pressure) within a reactor microchannel is determined by solving the following forms of the conservation of mass (continuity) and Navier-Stokes (momentum) equations:

$$\nabla \cdot \mathbf{V} = 0 \tag{1}$$

$$\rho \mathbf{V} \cdot \nabla \mathbf{V} = -\nabla p + \mu(\nabla^2 \mathbf{V}) + \rho \mathbf{g} \tag{2}$$

in which **V** is Cartesian velocity vector (m/s), ρ is bulk mixture density (kg/m^3), $\boldsymbol{p}$ is pressure (Pa), μ is bulk mixture absolute viscosity (N·s/m^2), and **g** is gravitational acceleration vector (m/s^2).

The steady-state concentration field is governed by

$$\mathbf{V} \cdot \nabla C_i - D_i \cdot \nabla^2 C_i = 0 \tag{3}$$

in which i is species indicator (one equation for each species), C_i is concentration of species i (M), and D_i is diffusivity of species i in solvent (m^2/s).

The kinetics of the heterogeneous chemical reaction that takes place at the solid-liquid interfaces is described using the traditional Michaelis-Menten model, which is often employed for enzyme catalysis and other biochemical reactions:

$$v = \frac{V_{\max}[S]}{k_m + [S]} \tag{4}$$

in which v is reaction rate (mol/[s·m^2]); [S] is substrate concentration at the solid surface (M); $V_{\max}$ is maximum reaction rate (mol/[s·m^2]), $V_{\max} = k_{cat}$ [E]; k_m is Michaelis constant (concentration that gives $v = V_{\max}/2$) (M); k_{cat} is turnover number (s^{-1}); and [E] is enzyme concentration at the solid surface (mol/m^2).

Boundary Conditions

The physical situations investigated in our study involve flow within rectangular microchannels with and without internal features. Accurate solution of the governing equations presented in the previous section requires that the appropriate boundary conditions be set. At the channel inlet, a uniform velocity distribution and substrate concentration were specified, and at the channel exit, a fixed pressure boundary condition was assigned. A no-slip boundary condition ($\mathbf{V} = 0$) was applied at all solid sur-

faces. If no enzyme is present on a solid surface, the concentration boundary condition is given by

$$D_s \frac{d[S]}{dn} = 0 \tag{5}$$

in which D_s is diffusivity of the substrate in the solvent (m^2/s) and n is distance in the direction normal to the solid surface (m).

If enzyme is present at the surface, the following boundary condition, which includes Michaelis-Menten kinetics, was applied to implement the steady, heterogeneous catalysis reaction:

$$-D_s \frac{d[S]}{dn} = \frac{V_{\max}[S]}{k_m + [S]} \tag{6}$$

Numerical Solution Method

The differential equations presented in section Governing Equations were solved numerically using the CFD-ACE+ computational package developed by CFD Research in Huntsville, AL *(13)*. CFD-ACE+ is a finite-volume-based code that employs a variation of the SIMPLEC (Semi-Implicit Method for Pressure-Linked Equations Corrected) algorithm *(14)*. As with all finite-volume methods, two major approximations are employed:

1. The physical domain is broken down into a series of small control volumes (cells). The resultant collection of cells is referred to as the computational grid.
2. The governing differential equations are replaced with a set of algebraic finite-difference equations that approximate the requirements of the differential equations on each cell.

Three-dimensional structured grids were developed for those cases in which internal features were not present within the reactor channels. For cases with internal features, unstructured grids were utilized.

The solution proceeds in two major steps. First, the velocities and pressures at the cell centers are calculated using an iterative pressure-correction approach (SIMPLEC). Once these flow field variables are determined, they are introduced into the approximated species conservation equation and the concentrations at the cell centers are calculated iteratively.

Prior Experimental Work

In a previous study *(7)*, tests were performed using a flow-through enzymatic microbioreactor to investigate the breakdown of urea into ammonia and carbon dioxide in the presence of urease (the enzyme catalyst). The chemical reaction is given by

$$NH_2CONH_2 + H_2O \xrightarrow{\text{urease}} 2NH_3 + CO_2 \tag{7}$$

The microreactor consisted of a series of parallel channels of rectangular cross-section. Each channel was 50 mm long, 500 μm wide, and 125 μm deep and contained triangular features. The construction material was PDMS, and urease was dispersed throughout the material prior to solidification. This produced a reasonably uniform concentration of entrapped enzyme at all solid surfaces. Reactors with three different enzyme mass concentrations (0.01, 0.02, and 0.03 g of urease/g of PDMS) were created. If the enzyme is assumed to be uniformly distributed in a cubic array throughout the PDMS, then a mass concentration of 0.01 g of urease/g of PDMS results in an enzyme surface concentration of approx 1.0×10^{11} mol/cm^2.

A reactant solution containing 0.1 mol/L of urea in water was fed to each microreactor using Cole Parmer Series 74900 syringe pumps, and the reactor effluent was analyzed by a Hewlett Packard 1100 HPLC (UV-Vis detector) and an Ocent Optics SD 2000 UV-Vis Spectrometer with fiberoptic flow analysis "Z" cells (FIA Lab). Flow was maintained for approx 1 h before operational data were recorded, to reduce the transient effects of enzyme washout. The resultant urea conversion efficiencies were determined for three different feed rates: 0.001, 0.006, and 0.06 mL/min *(7)*. The Reynolds numbers for these flow rates, based on the channel hydraulic diameter, are 0.041, 0.24, and 2.4, respectively.

Simulation Procedures and Results

Validation

Three-dimensional representations of a microreactor channel were created using CFD-ACE+, and simulations were performed to predict experimental destruction efficiencies. The reactor geometry and inlet conditions (flow rate and concentration) were set to match the experimental setup, and a portion of the computational grid is shown in Fig. 1. The unstructured grid consisted of approx 171,000 cells, a resolution that was found to give acceptable accuracy when compared with lower- and higher-resolution grids. All computations were performed on a Dell Dimension 4100 personal computer equipped with a 1.0-GHz Intel Pentium 3 processor and 1 GB of RAM. The computational times ranged between 2 and 8 CPU hours depending on Reynolds number (*Re*).

The fluid flow, mass transfer, and reaction kinetics parameters were taken from the open literature. The parameters that describe the nine validation cases are given in Tables 1 and 2. The very low Reynolds numbers ranging between 0.041 and 2.4 are again noted.

Figure 2 shows a typical velocity field solution. The small arrows scattered throughout the mid-plane flow field show the flow direction, and the shading indicates the magnitude of the axial velocity.

The experimental and computational results are shown graphically in Figs. 3–5. Figure 3 represents an enzyme concentration of 0.01 g of

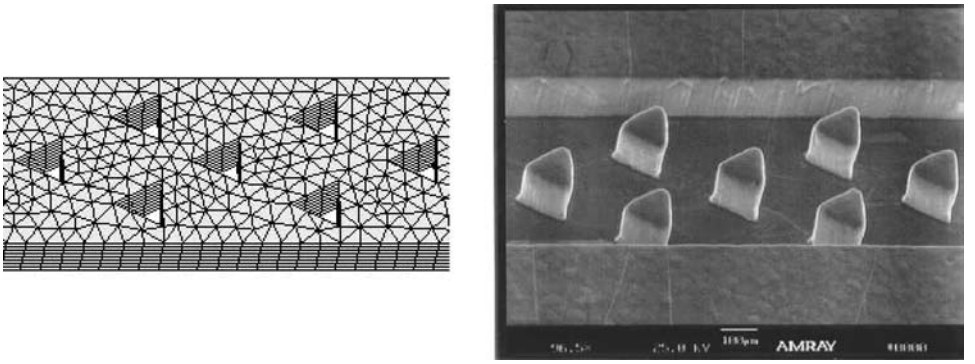

Fig. 1. Portion of computational grid used for validation, together with scanning electron microscope image of reactor channel.

Table 1
Flow, Mass Transfer, and Kinetics Parameters[a]

Property	Symbol	Value
Bulk mixture density *(15)*	ρ	998 kg/m^3
Bulk mixture kinematic viscosity *(15)*	ν	1.31×10^{-6} m^2/s
Diffusivity of urea in water (25°C) *(16)*	D_i	1.3×10^{-9} m^2/s
Michaelis constant for breakdown of urea catalyzed by urease *(17)*	k_m	0.025 *M*
Turnover number for breakdown of urea catalyzed by urease *(17)*	k_{cat}	1.0×10^4 s^{-1}

[a]A 0.1 *M* urea in water solution was used. The enzyme was urease.

Table 2
Flow and Concentration Parameters Defining Nine Validation Cases (Urea) *(7)*

Case	Volume flow rate (mL/min)	Inlet velocity (m/s)	*Re*	Urease concentration (g urease/g PDMS)
1	0.001	0.00027	0.041	0.01
2	0.006	0.0016	0.24	0.01
3	0.060	0.0160	2.4	0.01
4	0.001	0.00027	0.041	0.02
5	0.006	0.0016	0.24	0.02
6	0.060	0.0160	2.4	0.02
7	0.001	0.00027	0.041	0.03
8	0.006	0.0016	0.24	0.03
9	0.060	0.0160	2.4	0.03

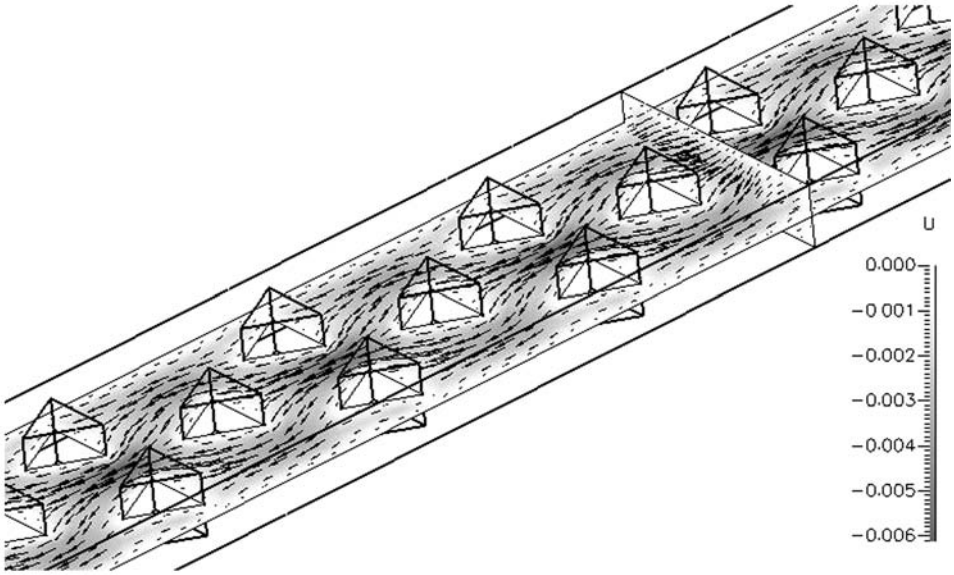

Fig. 2. Typical laminar velocity field for computational simulation (Re = 0.24). Negative values indicate that the flow is from right to left. Velocity is in meters per second.

urease/g of PDMS, which corresponds to an enzyme surface concentration of approx 1.0×10^{11} mol/cm^2. Figures 4 and 5 represent urease concentrations of 0.02 and 0.03 g of urease/g of PDMS, respectively.

In each figure, the solid triangles represent the experimental results for three flow rates of a 0.1 *M* urea in water solution. The volume flow rate, *Q* (milliliters/minute), is shown on the *x*-axis, and the percentage of urea destruction achieved in a single pass through the reactor (destruction efficiency, *DE*) is shown on the *y*-axis. The scales are logarithmic. A curve of best fit through the experimental data set is shown as a dashed line. As the flow rate increases, the residence time within the reactor channel decreases, and the urea has less time to react. The laminar flow patterns within the channel also change, and the net result is that, for a given enzyme concentration, the destruction efficiency decreases with increasing flow. By comparing Figs. 3–5, it is also seen that, at a given flow rate, increasing the enzyme concentration increases the destruction efficiency. Both of these results, which were reported in ref. *7*, are as expected.

Regarding the computational predictions, the solid squares in Figs. 3–5 represent the results of CFD-ACE+ simulations that assume that all enzymes on the reactor surface are active (100% activity). The upper solid lines are curve fits of these data. The solid diamonds and lower solid lines represent a simulation with 10% of the surface enzymes active. The active enzyme concentration at the solid-liquid interface has not been measured,

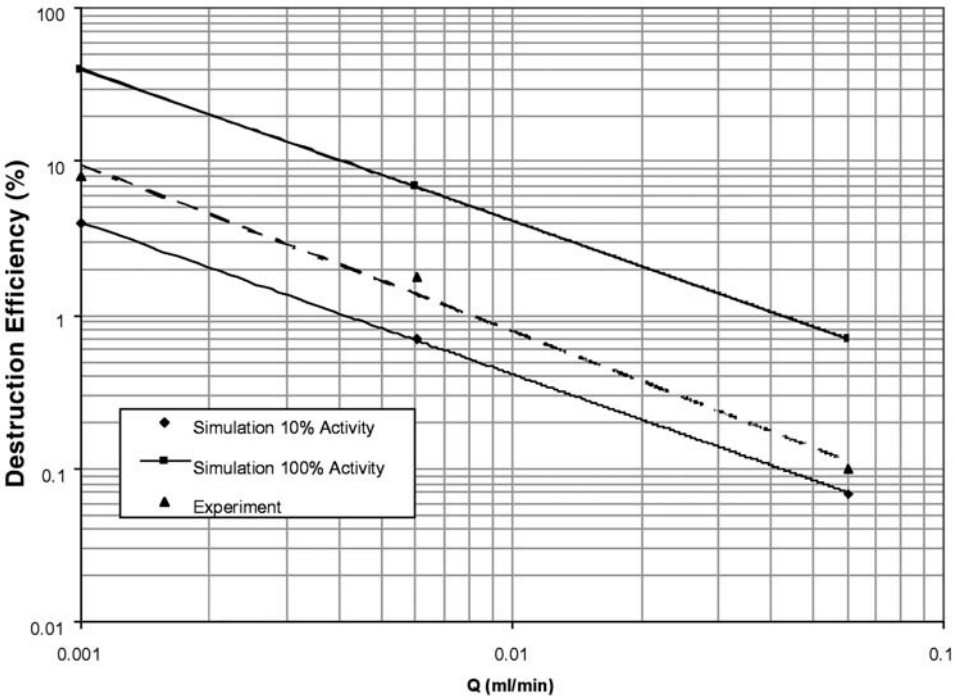

Fig. 3. Comparison of simulation and experimental results for destruction of urea (0.01 g of urease/g of PDMS).

but the simulations represent reasonable upper and lower bounds for this parameter.

For the range of data presented, the computational results are described very well by a power curve relationship between *DE* and *Q*, i.e., $DE = CQ^n$. The experimental results show more scatter about such a line. Two general observations are offered: (1) the overall trends exhibited by the experimental data are also present in the computational simulations, and (2) the computational simulations (100 and 10% activity) essentially bracket the experimental data.

No details of the flow and concentration fields were available from the experiments, so only a general comparison of overall reactor performance (destruction efficiency) can be made. Nevertheless, within this context, it is evident that the computational simulations yielded reasonable results and were able to capture the major trends in destruction efficiency. This is important because it is the capture of the proper trends that allows computational techniques to yield useful predictions even when extreme accuracy cannot be assured. That is, if the computational models predict the correct general effect of a design change, then they can be used to test a variety of such changes with good confidence that physical experimentation would yield similar qualitative results.

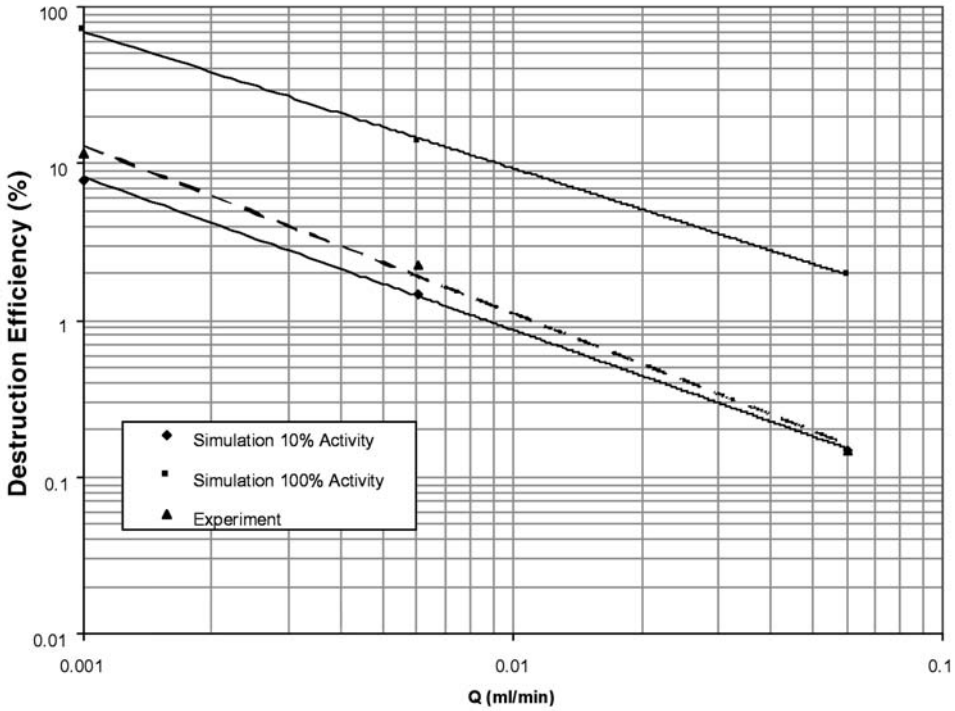

Fig. 4. Comparison of simulation and experimental results for destruction of urea (0.02 g of urease/g of PDMS).

Comparison of the computational and experimental results also allows the "effective" percentage of enzyme activity of the experimental test cases to be inferred; Table 3 summaries this information. A value of 100 % would indicate that the destruction efficiency measured for a particular test was equal to that predicted by CFD-ACE+ when a uniform dispersal of enzyme (with 100% activity) throughout the PDMS is assumed. Predictions of effective enzyme activity ranged from 9 to 26%. The results suggest that the percentage of active enzymes is significantly lower at the highest flow rate (0.06 mL/min).

Effect of Internal Features

Having shown that the computational approach is capable of predicting the trends present in experimental data, we undertook a second activity to demonstrate the use of this approach as a design tool. The reactors from the experimental studies contained internal triangular features to potentially improve the destruction efficiency by increasing the contact area and altering the laminar flow patterns. These features were included based on our intuition, without any quantitative evidence of their benefits. Therefore, as a simple design application, the computation approach was used to determine the impact of the features on destruction efficiency. Two

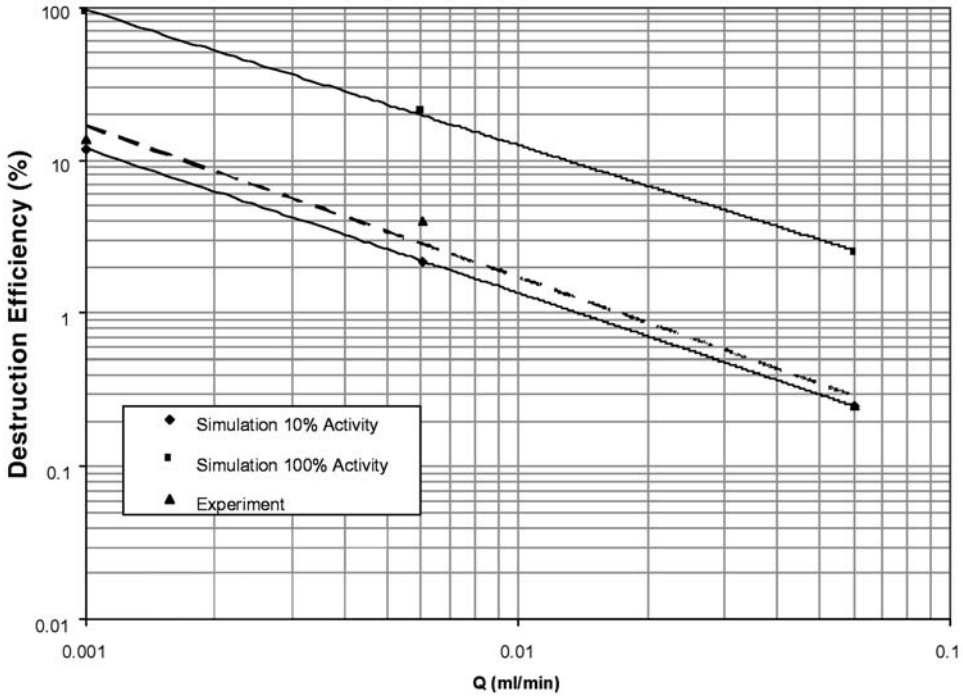

Fig. 5. Comparison of simulation and experimental results for destruction of urea (0.03 g of urease/g of PDMS).

Table 3
"Effective" Percentage of Enzyme Activity Inferred from Measured Destruction Efficiency and Computational Results

	Effective percentage of enzyme activity (%)		
Urease concentration (g/g PDMS)	0.001 mL/min	0.006 mL/min	0.06 mL/min
0.1	25	26	11
0.2	18	16	9
0.3	14	19	10

cases were considered: (1) a channel with no features, and (2) a channel with multiple triangular features. The computational grid with features present has already been shown in Fig. 1. The structured grid for the no-feature case is presented in Fig. 6. The cell sizes for the two cases were kept approximately equal.

Although the computational approach was validated using experimental data for the breakdown of urea into ammonia and carbon dioxide in the presence of urease, the equations used in the model are in no way limited to that specific enzyme/reaction combination, and the param-

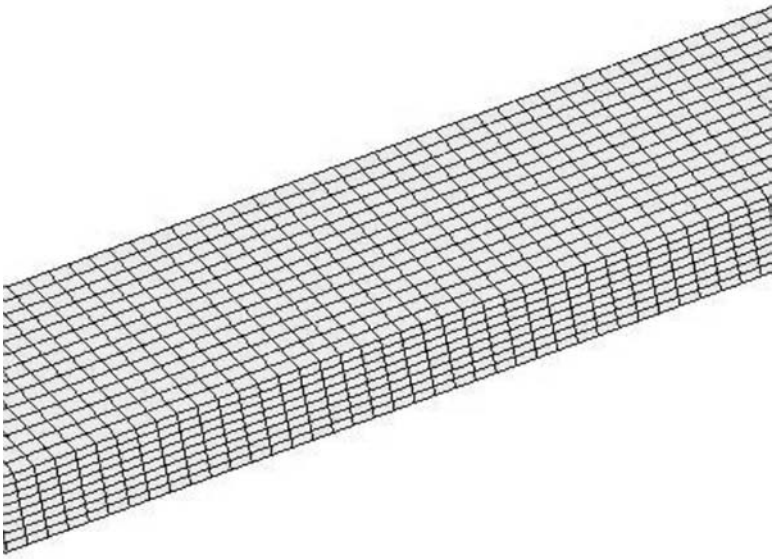

Fig. 6. Portion of computational grid for case without internal features.

eter values used in the simulations were taken from the open literature. The intent was to validate the method so that it could then be used for many different enzyme catalysis reactions. With that in mind, we selected a different enzyme/reaction combination for the feature study, namely, the breakdown of H_2O_2 into oxygen and water in the presence of catalase (the enzyme catalyst):

$$H_2O_2 \xrightarrow{\text{catalase}} H_2O + \frac{1}{2}O_2 \tag{8}$$

The fluid flow, mass transfer, and reaction kinetics parameters were again taken from the open literature and are provided in Table 4. An active catalase surface concentration of 1.0×10^{11} mol/cm^2 was assigned at all solid surfaces, including the channel "roof." The same volume flow rate (0.1 mL/min) and H_2O_2 inlet concentration (0.0147 *M*) were specified, and the destruction efficiency was calculated for each case. Since the "with-features" case provides approx 17% more surface area for reaction, it was expected to increase destruction efficiency significantly. However, the internal features also alter the flow pattern, so the actual change in destruction efficiency could not be predicted analytically.

The results of the simulations are shown in Figs. 7 and 8 and Table 5. The addition of internal features increased the destruction efficiency from 60 to 99%, a relative increase of 65%. This is in excess of the 17% increase in surface area, indicating that the changes in flow pattern induced by internal features can have a beneficial effect beyond that owing to increased surface area. The radically different concentration profiles shown in Fig. 8 illustrate

Table 4
Flow, Mass Transfer, and Kinetics Parameters[a]

Property	Symbol	Value
Bulk mixture density *(15)*	ρ	998 kg/m^3
Bulk mixture kinematic viscosity *(15)*	ν	1.31×10^{-6} m^2/s
Diffusivity of H_2O_2 in water	D_i	1.0×10^{-9} m^2/s
Michaelis constant for breakdown of H_2O_2 catalyzed by catalase *(17)*	k_m	0.025 M
Turnover number for breakdown of H_2O_2 catalyzed by catalase *(17)*	k_{cat}	1.0×10^7 s^{-1}

[a]A 0.0147 *M* H_2O_2 in water solution was used. The enzyme was catalase.

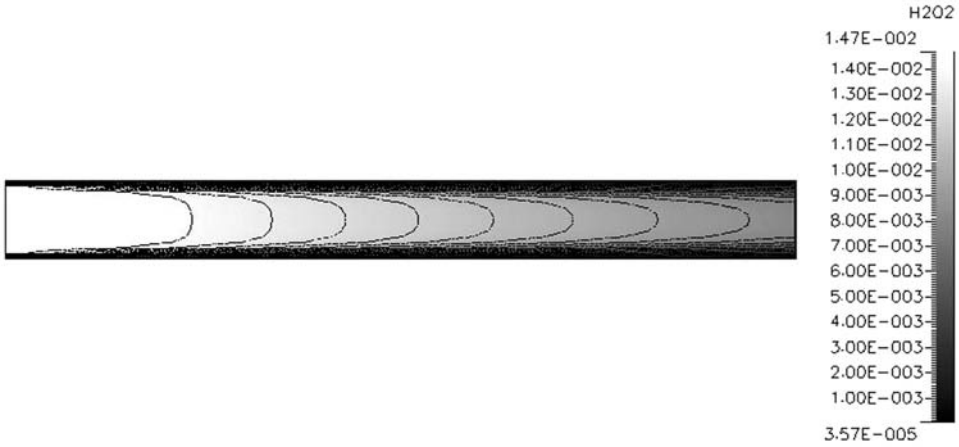

Fig. 7. H_2O_2 concentration (*M*) in channel midplane without features (view from above the channel; channel width enlarged by a factor of 10 for viewing).

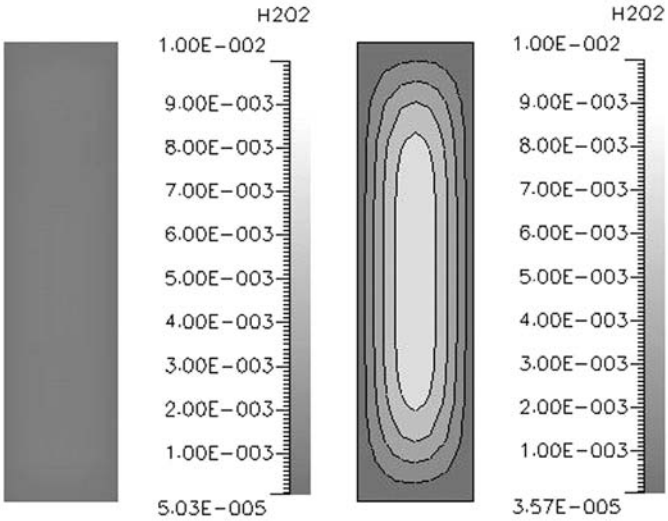

Fig. 8. H_2O_2 concentration (*M*) in channel exit plane (left) with features and (right) without features.

Table 5
H_2O_2 Destruction Efficiencies with and Without Internal Features
(Computational Results)

Without features (%)	With features (%)	Ratio
60	99	1.65

the effects of these changes in flow pattern. This is important because it suggests that modifying the reactor design by adding internal features can indeed improve overall performance of the reactor. Further, it implies that feature size, shape, location, and density may be optimized to produce a superior reactor design.

Such internal features do not come without a price, however. Their inclusion poses no significant challenges for the current manufacturing method, but they do result in an increased drop in pressure across the channels (0.53 psia with features vs 0.22 psi without features). This means that more energy is required to force the fluid through the reactor, and it can also lead to an increased likelihood of leakage or structural failure if reactors are operated at significantly higher flow rates.

Conclusion

The results of our study demonstrate that computational models can be used to predict destruction efficiencies within immobilized enzymatic bioreactors. Because it was found that the presence of internal features within the reactor channels enhanced the destruction efficiency more than could be attributed to the simple increase in surface area, additional studies are under way to optimize feature characteristics as well as other parameters such as channel size and mixture flow rate. In addition, avenues for increasing enzyme activity (and, hence, destruction efficiency) under the unique circumstances presented by these reactors are being examined.

Acknowledgment

We gratefully acknowledge the support of the University of Tennessee at Chattanooga Center of Excellence for Computer Applications.

References

1. Wegeng, R., Call, C., and Drost, K. (1996), *Chemical System Miniaturization*, PNNL-SA-27317, Pacific Northwest National Laboratory, Richland, WA.
2. Schuth, F. (1995), *Crystallographically Defined Pore Systems: Reaction Vessels with Molecular Dimensions*, *Microsystem Technology for Chemical and Biological Microreactors*, Max Planck Institute, Mainz, Germany.
3. Srinivasan, R., Hsing, I.-M., Berger, P. F., Jensen, K. F., Firebaugh, S. L., Schmidt, M. A., Harold, M. P., Lerou, J. J., and Ryley, J. (1997), *AIChE J.* **43(11),** 3059–3069.

4. Zheng, A.-P., Jones, F., Fang, J., and Cui, (2000), in *Proceedings of the 4th International Conference on Microreaction Technology (IMRET IV)*, Irven Rinard (Ed.), AIChE, Atlanta, GA, pp. 284–292.
5. Duffy, D. C., McDonald, J. C., Schueller, O. J. A., and Whitesides, G. M. (1998), *Anal. Chem.* **70,** 4974–4984.
6. Jones, F., Lu, Z., and Elmore, B. (2002), *Appl. Biochem. Biotechnol.* **98–100,** 627–640.
7. Jones, F., Forrest, S., Palmer, J., Lu, Z., Elmore, J., and Elmore, B. (2004), *Appl. Biochem. Biotechnol.* **113–116,** 261–272.
8. Mengeaud, V., Ferrigno, R., Josserand, J., and Girault, H. (2001), in *Microreaction Technology, IMRET 5: Proceedings of the Fifth International Conference on Microreaction Technology*, Springer-Verlag, New York, pp. 350–358.
9. Marioth, E., Loebbecke, S., Scholz, M., Schnürer, F., Türcke, T., Antes, J., and Krause, H. (2001), in *Microreaction Technology, IMRET 5: Proceedings of the Fifth International Conference on Microreaction Technology*, M. Matlosz, W. Ehrfeld, and J. P. Baselt (Eds.), Springer-Verlag, New York, pp. 262–274.
10. Heo, H. and Suh, Y. (2003), in *Proceedings of the First International Conference on Microchannels and Minichannels*, S. G. Kandlikar, G. P. Celata, S. Nishio, P. Stephan, B. Thonon (Eds.), American Society of Mechanical Engineers, New York, pp. 249–255.
11. Niklas, M. and Favre-Marinet, M. (2003), in *Proceedings of the First International Conference on Microchannels and Minichannels*, S. G. Kandlikar, G. P. Celata, S. Nishio, P. Stephan, B. Thonon eds., American Society of Mechanical Engineers, New York, pp. 335–342.
12. Barz, D. and Ehrhard, P. (2003), in *Proceedings of the First International Conference on Microchannels and Minichannels*, S. G. Kandlikar, G. P. Celata, S. Nishio, P. Stephan, B. Thonon eds., American Society of Mechanical Engineers, New York, pp. 365–371.
13. CDF Research Corporation. (2003), *CFD-ACE(U) User's Manual,* Huntsville, AL.
14. Van Doormaal, J. and Raithby, G. (1984), *Numer. Heat Transfer* **7,** 147–163.
15. Crowe, C., Roberson, J., and Elger, D. (2001), *Engineering Fluid Mechanics*, 7th ed., John Wiley & Sons, New York.
16. Sorrell, L. and Myerson, A., (1982), *AIChE J.* **28(5),** 772–778.
17. DeTurck, D., Gladney, L., and Pietrovito, A. (1996), *The Interactive Textbook of PFP 96*, http://dept.physics.upenn.edu/courses/gladney/mathphys/subsection4_1_7.html, University of Pennsylvania, Philadelphia.